



Radiation chemical studies of Gly-Met-Gly in aqueous solution

Sebastian Barata-Vallejo, Carla Ferreri, Tao Zhang, Hjalmar Permentier, Rainer Bischoff, Krzysztof Bobrowski & Chryssostomos Chatgililoglu

To cite this article: Sebastian Barata-Vallejo, Carla Ferreri, Tao Zhang, Hjalmar Permentier, Rainer Bischoff, Krzysztof Bobrowski & Chryssostomos Chatgililoglu (2016) Radiation chemical studies of Gly-Met-Gly in aqueous solution, Free Radical Research, 50:sup1, S24-S39, DOI: [10.1080/10715762.2016.1231402](https://doi.org/10.1080/10715762.2016.1231402)

To link to this article: <https://doi.org/10.1080/10715762.2016.1231402>



© 2016 The Author(s). Published by Informa UK Limited, trading as Taylor & Francis Group



Accepted author version posted online: 05 Sep 2016.
Published online: 25 Oct 2016.



Submit your article to this journal [↗](#)



Article views: 263



View related articles [↗](#)



View Crossmark data [↗](#)



Citing articles: 1 View citing articles [↗](#)

Radiation chemical studies of Gly-Met-Gly in aqueous solution

Sebastian Barata-Vallejo^{a*}, Carla Ferreri^a, Tao Zhang^b, Hjalmar Permentier^b, Rainer Bischoff^b, Krzysztof Bobrowski^{c†} and Chrysostomos Chatgililoglu^{a,d}

^aISOF, Consiglio Nazionale delle Ricerche, Bologna, Italy; ^bDepartment of Pharmacy, University of Groningen, Groningen, The Netherlands; ^cRadiation Laboratory, University of Notre Dame, Notre Dame, IN, USA; ^dInstitute of Nanoscience and Nanotechnology, NCSR Demokritos, Athens, Greece

ABSTRACT

Important biological consequences are related to the reaction of HO• radicals with methionine (Met). Several fundamental aspects remain to be defined when Met is an amino acid residue incorporated in the interior of peptides and proteins. The present study focuses on Gly-Met-Gly, the simplest peptide where Met is not a terminal residue. The reactions of HO• with Gly-Met-Gly and its *N*-acetyl derivative were studied by pulse radiolysis technique. The transient absorption spectra were resolved into contributions from specific components of radical intermediates. Moreover, a detailed product analysis is provided for the first time for Met-containing peptides in radiolytic studies to support the mechanistic proposal. By parallel radiolytical and electrochemical reactions and consequent product identification, the formation of sulfoxide attributed to the direct HO• radical attack on the sulfide functionality of the Met residue could be excluded, with the *in situ* generated hydrogen peroxide responsible for this oxidation. LC–MS and high resolution MS/MS were powerful analytical tools to envisage the structures of five products, thus allowing to complete the mechanistic picture of the overall Met-containing peptide reactivity.

ARTICLE HISTORY

Received 7 July 2016
Revised 15 August 2016
Accepted 28 August 2016

KEYWORDS

Methionine; free radicals; peptide; ionizing radiation; electrochemistry; EC-MS; LC–MS/MS; reaction mechanism





Introduction

The oxidation of methionine (Met) is an important reaction in the biological milieu. The major oxidation products by reactive oxygen species (ROS) are two epimeric forms of sulfoxide (i.e. *R* and *S* epimers) that can be repaired enzymatically by methionine sulfoxide reductase (Msr) [1,2]. Therefore, Met residues in proteins are suggested to act as an antioxidant pool and several studies support this hypothesis [3,4]. The reaction of oxidants like H₂O₂, HOONO, or HOCl with Met occurs in a site-specific manner with formation of methionine sulfoxide, Met(O) [5–7], whereas the oxidation by HO• radical is believed to be more complex [8].

Some of us recently reported the detailed product studies of the gamma-radiolysis of free Met (1) [9]. We disclosed that (i) HO• radicals and H• atoms are highly specific for sulfur atom attack under anoxic and aerobic conditions, (ii) HO• do not oxidize Met to the corresponding sulfoxide either in the presence or absence of oxygen, (iii) H• atom attack leads to the formation of


α -aminobutyric acid (2) or homoserine (3), in the absence or presence of oxygen, respectively, and (iv) H₂O₂ formed either from the radiolysis of water or from the disproportionation of the by-product O₂^{•-} is responsible for Met(O) formation. These reactions are summarized in Scheme 1 together with the reactive intermediates suggested by pulse radiolysis studies, i.e. the observed transient species assigned to a three-electron bond species 4 (the hydroxyl adducts immediately coordinate with nitrogen) which decay ($k_2 = 3.6 \times 10^6 \text{ s}^{-1}$) directly into CO₂ and an α -aminoalkyl radical (5) [10,11].

Although the reaction of HO• with free Met is well understood [9], several fundamental aspects remain to be defined when Met is a residue in peptides and proteins. Functional groups (neighboring groups) adjacent to the sulfur center, the primary site of initial oxidation, have clearly a key influence. Such neighboring group participation in the oxidation of Met not only stabilizes the corresponding radical cation (Met > S^{•+}) but may

CONTACT Chrysostomos Chatgililoglu  chrys@isof.cnr.it  ISOF, Consiglio Nazionale delle Ricerche, Via Piero Gobetti 101, 40129 Bologna, Italy; Krzysztof Bobrowski  k.bobrowski@ichtj.waw.pl  Institute of Nuclear Chemistry and Technology, Dorodna 16, 03-195 Warszawa, Poland

*Permanent address: Departamento de Química Orgánica, Facultad de Farmacia y Bioquímica, Universidad de Buenos Aires, Argentina

†Permanent address: Institute of Nuclear Chemistry and Technology, Dorodna 16, 03-195 Warszawa, Poland

 Supplemental data for this article can be accessed [here](#).

© 2016 The Author(s). Published by Informa UK Limited, trading as Taylor & Francis Group

This is an Open Access article distributed under the terms of the Creative Commons Attribution-NonCommercial NoDerivatives License (<http://creativecommons.org/licenses/by-nc-nd/4.0/>), which permits non-commercial re-use, distribution, and reproduction in any medium, provided the original work is properly cited, and is not altered, transformed, or built upon in any way.

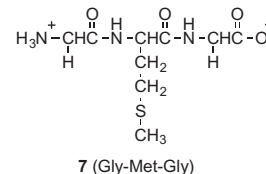
also render the reduction potential of Met less positive, and therefore facilitate its oxidation [12]. Moreover, the reactions of two intermediates, $\text{Met} > \text{S}^{\bullet+}$ and $\text{Met} > \text{S}:\cdot\text{OH}$ within particular peptide and protein domains are influenced by groups such as carboxylate, amino, hydroxyl, and amide functionalities [13–16].

So far, the formation of sulfoxide in the radiolytic study of model peptides under anaerobic conditions was attributed to HO^\bullet attack at the sulfur of Met residue [17–20]. It was also reported that sulfide radical cation complexes, $[\text{S}:\cdot\text{S}]^+$ and $[\text{S}:\cdot\text{N}]^+$, can form sulfoxide in oxygen-containing aqueous solution, either through reaction with superoxide or through a hydroxide-dependent reaction with molecular oxygen [21,22].

On the other hand, the reactivity of H^\bullet atoms with Met residues in peptides/proteins has been studied by some of us [23,24]. We showed that the reaction of H^\bullet atoms with peptides/proteins determines Met conversion into the non-genetically coded amino acid α -aminobutyric acid (Aba). We have identified this chemical mutation in Met-enkephalin [25], β -amyloid [26], bovine RNase A [27,28], human serum albumin [29], and various metalloproteins [30]. This reactivity has also been placed in a biomimetic context, since it has been suggested as molecular basis of the tandem protein–lipid damage [23,24]. Indeed, it was coupled with the formation of diffusible thiyl radicals originated from the protein desulfurization reactions. The methanethiyl radicals ($\text{CH}_3\text{S}^\bullet$) should be able to migrate from the aqueous to the membrane compartment and catalyze the double bond *cis*–*trans* isomerization process of the phospholipid unsaturated residues [31].

The present study focuses on the reaction of HO^\bullet radicals and/or H^\bullet atoms with Gly-Met-Gly (7), the simplest model peptide – where Met residue is internally located – to investigate differences with free Met. Identification and quantification of transient species

and final products has been provided.



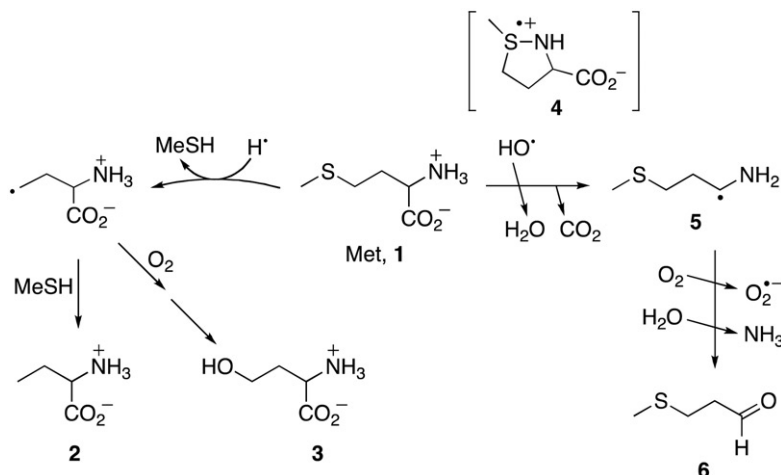
Materials and methods

Materials

Gly-Met-Gly as trifluoroacetate was obtained from Peptide 2.0 Inc. (Chantilly, VA) and used as received. Gly-Met-Gly and *N*-Ac-Gly-Met-Gly as free peptides were purchased from Bachem (Bubendorf, Switzerland). Orthophthaldialdehyde (OPA) perchloric acid (HClO_4), formic acid (HCOOH , FA, 98%) were purchased from Fluka-Sigma Aldrich Co. (Milan, Italy and Steinheim, Germany) and used without any further purification. 1-Palmitoyl-2-oleoyl-phosphatidylcholine (POPC) was obtained from Avanti Polar Lipids (Alabaster, AL) and used as received. Acetonitrile (HPLC SupraGradient grade) was purchased from Biosolve (Valkenswaard, The Netherlands). Other solvents (HPLC grade) were purchased from Merck Millipore (Darmstadt, Germany) and used without further purification. All solutions were made with deionized water (18 M Ω resistance) provided by a Millipore MilliQ system (conductivity 18.2 M Ω cm, Millipore Corp., Billerica, MA). All aqueous peptide solutions were prepared immediately before use.

Pulse radiolysis

Experiments were performed with the Notre Dame Titan 8 MeV Beta model TBS 8/16-15 linear accelerator with typical pulse lengths of 2–10 ns. The data acquisition system allows for kinetic traces to be displayed on



Scheme 1. HO^\bullet radicals and H^\bullet atoms are highly specific for sulfur atom attack of methionine (1).

multiple time scales. A detailed description of the experimental setup for optical measurements has been given elsewhere along with the basic details of the equipment and the data collection system [32]. Absorbed doses per pulse were of the order of 4–8 Gy (1 Gy equals 1 J kg⁻¹). For time-resolved measurements of optical spectra, N₂O-saturated solutions containing 10⁻² M KSCN were used as the dosimeter, with a radiation chemical yield of $G = 0.635 \mu\text{mol J}^{-1}$ and a molar absorption coefficient of $7580 \text{ dm}^3 \text{ mol}^{-1} \text{ cm}^{-1}$ at 472 nm for the (SCN)₂^{•-} radical [33]. The SI units ($\mu\text{mol J}^{-1}$) for radiation chemical yield, G , are the concentrations of radicals (in micromoles) produced per joule of energy absorbed. The pH of ~5.5 was recorded for N₂O-saturated solutions of 0.2 mM Gly-Met-Gly or *N*-Ac-Gly-Met-Gly as free peptides. The pH 1 was adjusted by adding HClO₄. Solutions were purged for at least 30 min per 500 mL sample with the appropriate gas (N₂O or N₂) before pulse irradiation. Experiments were performed with a continuous gas flow of the solutions at room temperature (23 °C). Experimental error limits are 10% unless specifically noted.

Resolution of time-resolved spectra

Optical spectra, monitored at various time delays following the electron pulse, were resolved into specific components (representing individual transients) by linear regression according to the following equation [34]:

$$G \times \varepsilon(\lambda_j) = \sum_{i=1}^n G_i \times \varepsilon(\lambda_j)$$

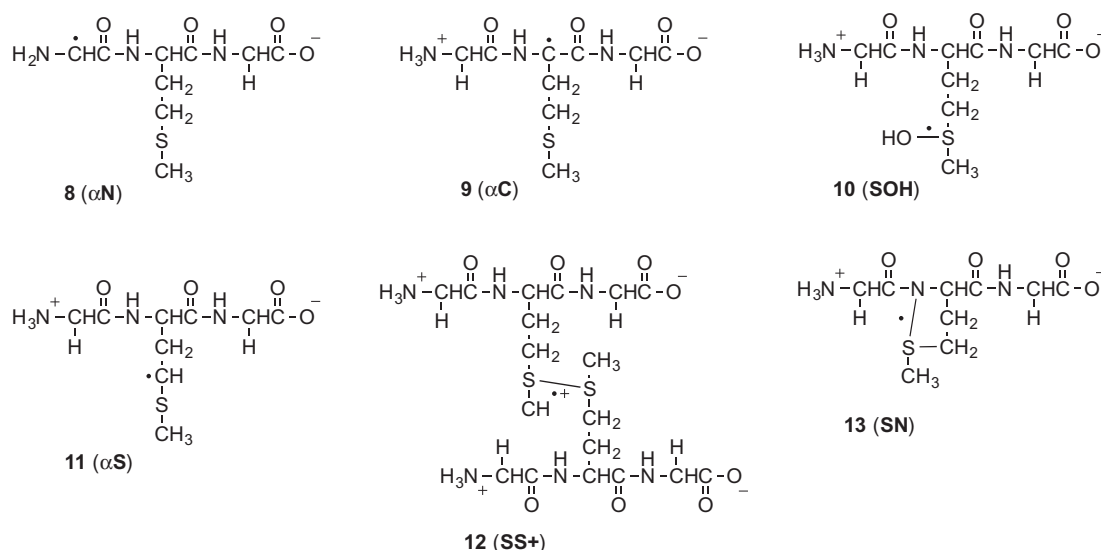
Here, $G \times \varepsilon(\lambda_j)$ is equal to the observed absorbance change $\Delta A(\lambda_j)$ of the composite spectrum multiplied by the factor (F) from the dosimetry. $F = \varepsilon_{472} \times G((\text{SCN})_2^{\bullet-}) /$

ΔA_{472} where ε_{472} is the molar extinction coefficient of (SCN)₂^{•-} at 472 nm, $G((\text{SCN})_2^{\bullet-})$ is the radiation chemical yield of the (SCN)₂^{•-} radicals, and ΔA_{472} represents the observed absorbance change at 472 nm in the thiocyanate dosimeter. G_i is the linear regression coefficient of the i th species and $\varepsilon(\lambda_j)$ is the molar extinction coefficient of the i th species, and the j th wavelength. Further details of this method have been described elsewhere [35].

Several criteria were applied to validate the spectral resolutions and to eliminate unreasonable fits: (i) within $\pm 15\%$, the combined yields of the transient species derived from their respective extinction coefficients cannot exceed the initial radiation chemical yield of the primary species, i.e. $G_i(\text{HO}^\bullet) = 0.60 \mu\text{mol J}^{-1}$ (at pH 5.5) or $0.29 \mu\text{mol J}^{-1}$ (at pH 1). The error limit of $\pm 15\%$ allows for a $\pm 5\%$ variation in the experimental data and a $\pm 10\%$ combined error in the reported molar absorption coefficients for the UV spectra of the components under consideration. (ii) The radiation chemical yields of the respective species (Scheme 2) in the optical spectra were calculated taking the following representative molar absorption coefficients (units in $\text{dm}^3 \text{ mol}^{-1} \text{ cm}^{-1}$): $\varepsilon_{340}(\text{SOH}) = 3400$ [36], $\varepsilon_{390}(\text{SN}) = 4500$ [37], $\varepsilon_{480}(\text{SS}^+) = 6900$ [38], $\varepsilon_{290}(\alpha\text{S}) = 3000$ [39], $\varepsilon_{260}(\alpha\text{N}) = 3300$ [11], and $\varepsilon_{270}(\alpha\text{C}) = 6200$, $\varepsilon_{370}(\alpha\text{C}) = 1800$ [40].

Steady-state γ -radiolysis

Irradiations were performed at room temperature using a ⁶⁰Co-Gammacell at different dose rates. The exact absorbed radiation dose was determined with the Fricke chemical dosimeter, by taking $G(\text{Fe}^{3+}) = 1.61 \mu\text{mol J}^{-1}$ [41]. Mixtures of gases were obtained by



Scheme 2. Reactive intermediates discussed in the resolution of time-resolved spectra.

an appropriate mixer, controlled by a flow meter connected to the line, reaching the vessel through a needle. The flow was adjusted to get a continuous bubbling during irradiation. Four milliliters of a N_2 -purged aqueous solution of Gly-Met-Gly as trifluoroacetate (all experiments were run at 1 mM peptide concentration and at natural pH) (pH value of ~ 6.8 was recorded) was saturated with the desired gas or gas mixture prior to γ -irradiation.

OPA derivatization of irradiated samples and HPLC analysis

HPLC analyses were recorded on an Agilent 1100 Liquid Chromatograph, equipped with a quaternary pump delivery system, a column thermostat, and a variable-wavelength detector. RP18 $5\ \mu\text{m}$ columns were used in the HPLC analyses. Aliquots of the irradiated Gly-Met-Gly solutions were withdrawn at the specified doses for immediate conversion to the OPA (orthophthalaldehyde) derivatives following a protocol previously published by our group [9].

Electrochemical oxidation and EC-MS analysis

Twenty micromolars of Gly-Met-Gly (GMG) was prepared in 89/10/1 (v/v/v) ultrapure water/acetonitrile/formic acid and oxidized in a thin-layer cell (Flexcell, Antec Leyden, Leiden, The Netherlands) with a Magic Diamond (BDD) working electrode (8 mm diameter, surface area $50.3\ \text{mm}^2$) and a palladium (Pd/H_2) reference electrode (Hy-REF) at a flow rate of $5\ \mu\text{L}/\text{min}$. Pretreatment of BDD electrodes was performed according to Roeser et al. [42]. Mass voltammograms of GMG were recorded on-line by ramping the cell potential linearly from 0 to 4000 mV at a scan rate of $20\ \text{mV}/\text{s}$ using a homemade potentiostat controlled by a MacLab system (ADInstruments, Castle Hill, NSW, Australia) and EChem software (eDAQ, Denistone East, NSW, Australia). The electrochemical oxidation products were analyzed using an API365 triple quadrupole mass spectrometer (MDS-Sciex, Concord, Ontario, Canada) upgraded to EP10+ (Ionics, Bolton, Ontario, Canada).

HPLC-MS/MS measurements

Liquid chromatography was performed on an Acquity UPLC system (Waters, Milford, MA) equipped with an Alltima HP HILIC column ($150\ \text{mm} \times 2.1\ \text{mm}$ i.d., $3\ \mu\text{m}$ particles, $120\ \text{\AA}$ pore size, Grace Alltech, Lokeren, Belgium) at a flow rate of $400\ \mu\text{L}/\text{min}$. Mobile phase A consisted of ultra-pure water with 0.1% formic acid. Mobile phase B was acetonitrile with 0.1% formic acid.

Twenty-five microliters of $100\ \mu\text{M}$ samples was injected, and separation was achieved with a gradient of 2–50% A in 25 min. The column was directly coupled to a Maxis plus quadrupole time-of-flight mass spectrometer (QTOF) (Bruker, Billerica, MA) for product detection in positive ion mode. High-resolution MS/MS experiments of reaction products of Gly-Met-Gly were performed in auto MS/MS mode (2 GHz) with a maximum of seven precursors per cycle and an active exclusion of 0.1 min using a mass range of 100–300 amu with a capillary voltage of 3500 V.

Results and discussion

Reactions of HO^\bullet with Gly-Met-Gly in aqueous solution: time-resolved spectra and analysis

The reaction of HO^\bullet with Gly-Met-Gly was investigated in $N_2\text{O}$ -saturated solution of $0.2\ \text{mM}$ Gly-Met-Gly at natural pH (pH value of 5.5 was recorded). A transient spectrum obtained $1.4\ \mu\text{s}$ after the electron pulse exhibits a strong UV band having $\lambda_{\text{max}}=270\ \text{nm}$ with $G \times \varepsilon_{270} = 1828\ \mu\text{mol}\ \text{J}^{-1}\ \text{dm}^3\ \text{mol}^{-1}\ \text{cm}^{-1}$ and a very weak and broad, almost flat, shoulder in the range 400–500 nm (\circ symbols in Figure 1). This spectrum can be resolved into contributions from the following components (cf. Scheme 2): the C^α -centered radicals (αC), the α -amino type radicals (αN), the α -(alkylthio)alkyl radicals (αS), the intermolecular sulfur-sulfur three-electron-bonded radical cations (SS^+), and the intramolecular sulfur-nitrogen three-electron-bonded radical (SN) with the respective G -values: 0.052, 0.34, 0.14, 0.029, and $0.035\ \mu\text{mol}\ \text{J}^{-1}$ (Table 1). The sum of all component spectra with their respective yields resulted

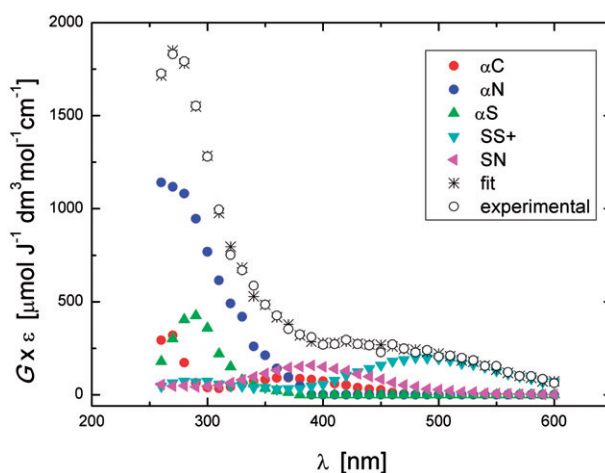


Figure 1. Resolution of the spectral components in the transient absorption spectrum recorded $1.4\ \mu\text{s}$ after the electron pulse in $N_2\text{O}$ -saturated aqueous solution containing $0.2\ \text{mM}$ Gly-Met-Gly at pH 5.5 (the explanation of symbols is in the legend and Scheme 2).

in a good fit (λ symbols in Figure 1) to the experimental spectrum. The total G -value ($0.60 \mu\text{mol J}^{-1}$) is in a very good agreement with the expected yield of HO^\bullet radicals available for the reaction with Gly-Met-Gly peptide at this pH. It is worthwhile to note that the HO^\bullet adduct to the sulfur atom (SOH) is not included in the spectral mix, which means that its life-time is shorter. This observation can be rationalized, by analogy to similar findings for S-methylglutathione [43], in terms of a concerted process which involves a fast proton transfer from the terminal $-\text{NH}_3^+$ group to S-O moiety, by which elimination of HO^- (in the form of water) occurs and leads to the intramolecularly bonded species $[\text{>S}:\text{NH}_2]^+$ **14** (Scheme 3). The radical cation **14** can give radical **8** through the sequential steps described in Scheme S1 (see Supporting Information). The reducing ability of radical **8** may play an important role in the product outcome (see discussion for Scheme 6).

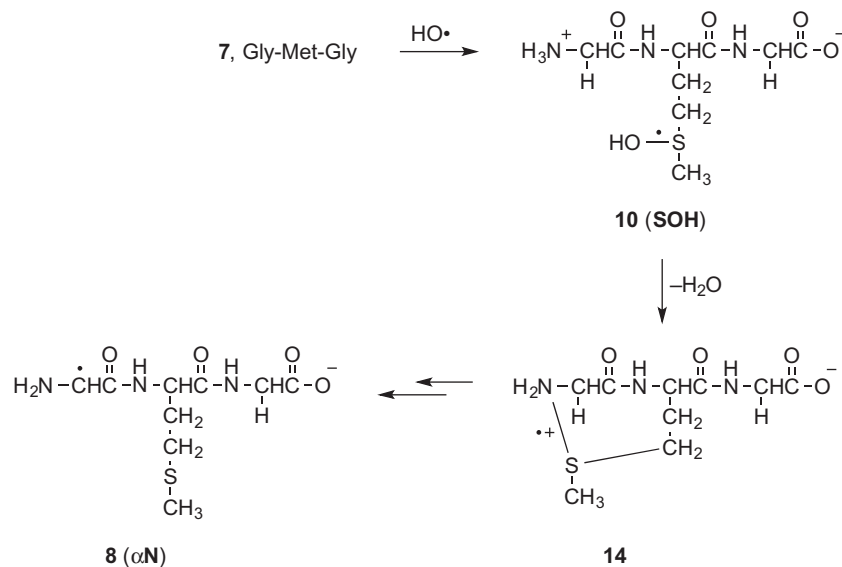
After $3.5 \mu\text{s}$, the transient absorption spectrum did not change much and it was still dominated by a distinct absorption band with the pronounced maximum at $\lambda = 270 \text{ nm}$ with the $G \times \epsilon = 1844$. In Table 1, G -values of radicals are collected together with their percentage contribution to the total yield of HO^\bullet radicals present in the Gly-Met-Gly system at different times after electron pulse. It is worthy to note that the most abundant radicals present in the irradiated Gly-Met-Gly system at short times after delivery of the electron pulse are αN and αS , which constitute more than 80% of all radicals. The transient spectrum obtained $75 \mu\text{s}$ after the electron pulse exhibited a broad uncharacteristic absorption band which shows no distinct $\lambda_{\text{max}} > 260 \text{ nm}$

with $G \times \epsilon_{260} = 1103 \mu\text{mol J}^{-1} \text{ dm}^3 \text{ mol}^{-1} \text{ cm}^{-1}$. This spectrum was resolved into contributions from αC , αN , and SS^+ (Table 1).

The purpose of decreasing pH of the reaction environment to pH 1 was to test whether the elimination of HO^- from the $>\text{S}:\text{OH}$ moiety by using external protons can compete with a fast proton transfer from the terminal $-\text{NH}_3^+$ group to the same moiety (cf. reaction **10**→**14** in Scheme 3). Detailed results are reported in Supporting Information (Figures S1–S3 and Table S1). A transient spectrum, obtained $1.4 \mu\text{s}$ after the electron pulse in N_2 -saturated solutions containing 0.2 mM of Gly-Met-Gly at pH 1, exhibited a strong UV band having $\lambda_{\text{max}} = 290 \text{ nm}$ and a second broad band in the range $440\text{--}500 \text{ nm}$ with weakly pronounced maximum at $\lambda \approx 480 \text{ nm}$. The respective $G \times \epsilon$ values were 634 and $311 \mu\text{mol J}^{-1} \text{ dm}^3 \text{ mol}^{-1} \text{ cm}^{-1}$ (see Figure S1). This spectrum was resolved into contributions from the components αN , αS , SS^+ , and SN using G -values 0.053 , 0.11 , 0.040 , and $0.029 \mu\text{mol J}^{-1}$, respectively. The calculated percentage contribution of the αN radicals to the total yield of HO^\bullet present at pH 1 is substantially lower

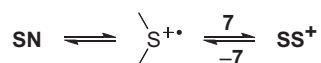
Table 1. The radiation chemical yields (G , $\mu\text{mol J}^{-1}$) of radicals and their percentage contribution (in parenthesis) to the total yield of radicals present in the reaction of HO^\bullet with Gly-Met-Gly at different times after electron pulse at pH 5.5.

Time, μs	αC	αN	αS	SS^+	SN
1.4	0.052 (8.6%)	0.34 (57.1%)	0.14 (23.6%)	0.029 (4.8%)	0.035 (5.9%)
3.5	0.061 (10.2%)	0.35 (58.7%)	0.13 (21.8%)	0.027 (4.5%)	0.029 (4.8%)
75	0.052 (20.8%)	0.19 (78.3%)	0	0.002 (0.8%)	0



Scheme 3. Suggested mechanism for the formation of αN from the HO^\bullet radical adduct to the sulfur atom (SOH) (see Scheme S1 for details)).

than that calculated at pH 5.5 (cf. Table S1 with Table 1). This observation can be rationalized in terms of the existence of two competitive reactions (cf. Scheme S1), the formation of $>S^{+\bullet}$ being more efficient at pH 1 than at pH 5.5, which is also reflected in the higher calculated percentage contribution of the αS radicals to the total yield of HO^\bullet present at pH 1, in comparison to pH 5.5. After 3.5 μs , the transient absorption spectrum was dominated by two distinct absorption bands with the pronounced maxima at $\lambda = 290$ nm and 490 nm with the respective $G \times \varepsilon$ of 756 and 466 (see Figure S2). This spectrum was resolved into contributions from the components αC , αN , αS , and SS^+ using G -values 0.021, 0.019, 0.16, and 0.068 $\mu mol J^{-1}$, respectively. The total G -value (0.26 $\mu mol J^{-1}$) is slightly lower than the expected yield of HO^\bullet radicals available for the reaction with Gly-Met-Gly at this pH. Interestingly, the comparison of the radiation chemical yields of the SN radicals and SS^+ radical cations measured at 1.4 and 3.5 μs after the pulse (Table S1) suggested that increase of $G(SS^+)$ occurs at the expense of decrease of $G(SN)$. This observation can be rationalized by the existence of two equilibria presented in Scheme 4. The transient spectrum obtained 150 μs after the electron pulse exhibits a broad uncharacteristic absorption band which shows no distinct $\lambda_{max} > 260$ nm with $G \times \varepsilon_{260} = 456 \mu mol J^{-1} dm^3 mol^{-1} cm^{-1}$ (Figure S3). This spectrum was resolved into contributions from the components αC , αS , and SS^+ using G -values 0.043, 0.074, and 0.002 $\mu mol J^{-1}$, respectively.



Scheme 4. The partition of the radical cation on Met moiety in two equilibria.

Reactions of HO^\bullet with *N*-Ac-Gly-Met-Gly in aqueous solution: time-resolved spectra and analysis

The purpose of acetylation of the *N*-terminal group in Gly-Met-Gly was to have another model of internally located Met, eliminating the fast proton transfer from free amino group to the $>S:OH$ moiety. This process was before suggested as the main decay reaction pathway of the $S-OH$ adduct in Gly-Met-Gly (cf. Scheme 3). A transient spectrum, obtained 1.5 μs after the electron pulse in N_2O -saturated solutions containing 0.2 mM *N*-Ac-Gly-Met-Gly at natural pH (pH value of 5.4 was recorded), exhibited a strong UV band having $\lambda_{max} = 290$ nm, a broad shoulder in the range 320–390 nm, and two shoulders in the range 400–550 nm (\circ symbols in Figure 2), suggesting the superposition of absorption spectra of several transient

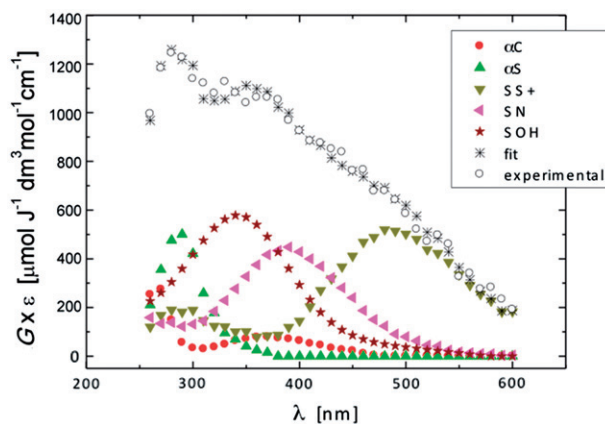


Figure 2. Resolution of the spectral components in the transient absorption spectrum recorded 1.4 μs after the electron pulse in N_2O -saturated aqueous solution containing 0.2 mM *N*-Ac-Gly-Met-Gly at pH 5.4 (the explanation of symbols is in the legend and Scheme 2).

Table 2. The radiation chemical yields ($G, \mu mol J^{-1}$) of radicals and their percentage contribution (in parenthesis) to the total yield of radicals present in the reaction of HO^\bullet with *N*-Ac-Gly-Met-Gly at different times after electron pulse at pH 5.4.

Time, μs	SOH	αC	αN	αS	SS^+	SN
1.4	0.18 (30.6%)	0.047 (8.1%)	0	0.17 (29.9%)	0.079 (13.6%)	0.10 (17.7%)
3.75	0.07 (11.8%)	0.023 (3.8%)	0	0.29 (49.0%)	0.097 (16.3%)	0.11 (19.2%)
7	0.058 (9.7%)	0.024 (3.9%)	0	0.32 (53.6%)	0.095 (15.9%)	0.10 (16.9%)

species. This spectrum can be resolved into contributions from the following components: SOH , αC , αS , SS^+ , and SN with the respective G -values: 0.18, 0.047, 0.17, 0.079, and 0.10 $\mu mol J^{-1}$ (Table 2). The sum of all component spectra with their respective yields resulted in a good fit (\circ symbols in Figure 2) to the experimental spectrum. The total G -value (0.58 $\mu mol J^{-1}$) was slightly lower than the expected yield of HO^\bullet available for the reaction with *N*-Ac-Gly-Met-Gly at this pH. This could be understood since at this time, the reaction of HO^\bullet with the *N*-Ac-Gly-Met-Gly is about to be completed. It is worthy to note that αN was not taken in the spectral mix.

A transient spectrum obtained 3.75 μs after the electron pulse exhibited a strong distinct UV band having $\lambda_{max} = 290$ nm, and a broad, almost flat, shoulder in the range 350–500 nm (\circ symbols in Figure 3). A good spectral resolution was obtained for this spectrum taking into account contributions from the same species: SOH , αC , αS , SS^+ , and SN with the respective G -values: 0.07, 0.023, 0.29, 0.097, and 0.11 $\mu mol J^{-1}$ (Table 2). The sum of all component spectra with their respective yields

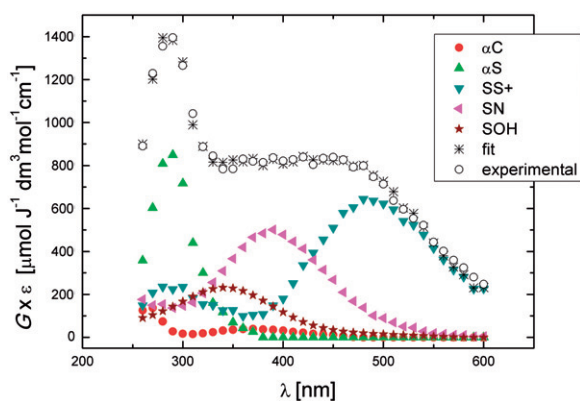


Figure 3. Resolution of the spectral components in the transient absorption spectrum recorded 3.75 μs after the electron pulse in N_2O -saturated aqueous solution containing 0.2 mM *N*-Ac-Gly-Met-Gly at pH 5.4 (the explanation of symbols is in the legend and Scheme 2).

resulted in a good fit to the experimental spectrum (à symbols in Figure 3). The total G -value ($0.60 \mu\text{mol J}^{-1}$) was in agreement with the expected yield HO^\bullet available for the reaction with *N*-Ac-Gly-Met-Gly at this pH. It is again worthy to note that αN radicals were not taken in the spectral mix. The most abundant radicals present in the irradiated *N*-Ac-Gly-Met-Gly system at 1.4 μs after the electron pulse are **SOH** and αS , which constitute more than 60% of all radicals (Table 2). The high yield of the $>\text{S}:\text{OH}$ radicals in the *N*-Ac-Gly-Met-Gly confirmed that in the previous nonacetylated NH_2 -substrate the fast proton transfer process from the *N*-terminal group occurred, which is responsible for the fast decay of the $>\text{S}:\text{OH}$ in Gly-Met-Gly not observed here. Moreover, the **SS**⁺ and **SN** constituted more than 30% of all radicals, this value being threefold higher than that in Gly-Met-Gly. With further time evolution, the most abundant radicals present at 3.75 and 7 μs after delivery of the electron pulse were the αS , which constitute nearly 50% of all radicals (Table 2). An increase of the G -values observed in this time domain for αS radicals occurs mostly at the expense of decrease of the $>\text{S}:\text{OH}$ radicals.

Product studies from the continuous γ -radiolysis of aqueous solutions of Gly-Met-Gly

The products resulting from the continuous γ -radiolysis of aqueous solutions of Gly-Met-Gly in the absence and presence of oxygen were investigated. In addition, the reaction of Gly-Met-Gly with H_2O_2 , simulating the steady-state formation of H_2O_2 during γ -irradiation, was examined in order to have a better understanding of the radiolysis outcome and the reactive species involved in the formation of the each product. Two approaches to analyze the reaction mixtures were

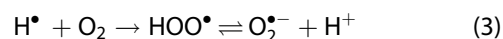
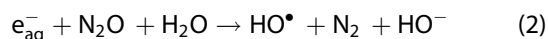
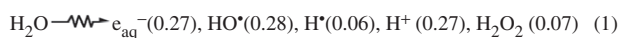
followed: (a) the OPA derivatization taking into account that this reagent is able to react with amino-containing moieties [44,45], followed by HPLC analysis; (b) the direct LC/MS analysis coupled with high-resolution MS/MS spectra to determine product structures. It is worth noting that the product analysis of Met-containing peptides has never been provided in radiolytic studies, and so far mechanistic schemes have been proposed without evidence from product identification.

Reaction of Gly-Met-Gly with H_2O_2

Five hundred microliters of 0.2 M aqueous H_2O_2 were introduced by syringe pump (flow rate 167 $\mu\text{L/h}$) to an aqueous solution of Gly-Met-Gly (25 mL, 10.10 mM, pH 6.8) under stirring for 3 h (H_2O_2 final concentration = 3.9 mM). Samples were withdrawn each hour, followed by OPA derivatization of amino compounds, and HPLC analysis. The oxidation of Gly-Met-Gly to Gly-Met(O)-Gly (**15**) occurs readily and quantitatively with respect to consumed starting tripeptide (see Figure 4). The samples withdrawn each hour during the experiment were also analyzed by ESI-MS direct insertion (positive mode), verifying the presence of two compounds in the reaction mixture: m/z 264.1 corresponding to Gly-Met-Gly +1 and m/z 280.1 corresponding to Gly-Met(O)-Gly +1. Analogous experiments were also performed where superoxide radical anions ($\text{O}_2^{\bullet-}$) are generated as the exclusive reactant upon γ -irradiation of O_2 -saturated aqueous. The reactivity of $\text{HO}_2^\bullet/\text{O}_2^{\bullet-}$ in aqueous solution is fully understood, and disproportionation is expected to produce H_2O_2 [46]. The details of these experiments are reported in Supporting Information.

Reaction of HO^\bullet radical and H^\bullet atom with Gly-Met-Gly in oxygenated aqueous solution

Radiolysis of neutral water leads to the reactive species e_{aq}^- , HO^\bullet , and H^\bullet together with H^+ and H_2O_2 as shown in reaction 1. The values in parentheses represent the radiation chemical yields (G) in units of $\mu\text{mol J}^{-1}$. In 1 atm of $\text{N}_2\text{O}:\text{O}_2$ (90:10 v/v) e_{aq}^- is efficiently transformed into HO^\bullet radicals via reaction 2 ($k_2 = 9.1 \times 10^9 \text{ M}^{-1} \text{ s}^{-1}$), affording $G(\text{HO}^\bullet) = 0.55 \mu\text{mol J}^{-1}$ [47,48], whereas 20% of the H^\bullet are transformed into $\text{O}_2^{\bullet-}$ (reaction 3).



$\text{N}_2\text{O}:\text{O}_2$ (90:10 v/v) saturated solutions containing Gly-Met-Gly (1.10 mM) at natural pH were irradiated

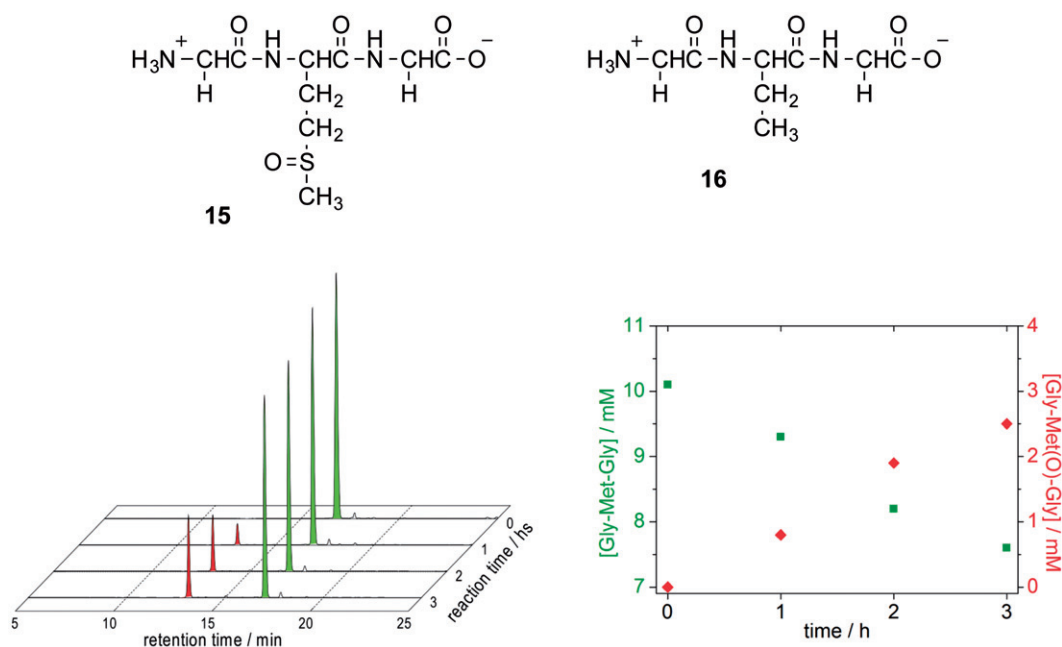


Figure 4. (A) HPLC traces showing the oxidation of Gly-Met-Gly (green peak) to Gly-Met(O)-Gly (red peak) by H_2O_2 . Samples were withdrawn every hour, followed by OPA derivatization (detecting amino compounds) and HPLC analysis. (B) Time course of the conversion of Gly-Met-Gly (■) into Gly-Met(O)-Gly (◆).

under steady state conditions with a dose rate of ca. 5.5 Gy min^{-1} , continuously bubbling the gas mixture throughout the irradiation time. Aliquots were taken at specified doses followed by OPA treatment [9], that reacts with amino-containing compounds, and HPLC analysis. The consumption of Gly-Met-Gly (green peaks, Figure 5) led to the formation of five products, two major and three minor ones. The product that eluted as the second one from the column ($R_t = 12.9 \text{ min}$, red peaks) was identified as Gly-Met(O)-Gly by comparison with the corresponding OPA derivatives obtained from Gly-Met-Gly oxidation by H_2O_2 . The analysis of the data in terms of chemical radiation yields for the consumption of Gly-Met-Gly and formation of the products bearing a primary amine functionality detectable by the OPA – HPLC technique are shown in Table 3 (see also Figure S5). It is worth mentioning that the G of disappearance of starting material is -0.640 whereas the sum of G values of the products is 0.601 . The results evidence one of the two possibilities: (i) only formation of products that maintain the amine functionality or (ii) products that lose the amine functionality together with other containing the amine moiety generated by chain processes.

Reaction of HO^\bullet radical and H^\bullet atom with Gly-Met-Gly in deaerated aqueous solution

In N_2O -saturated solution ($\sim 0.02 \text{ M}$ of N_2O), e_{aq}^- are efficiently transformed into HO^\bullet radicals, affording

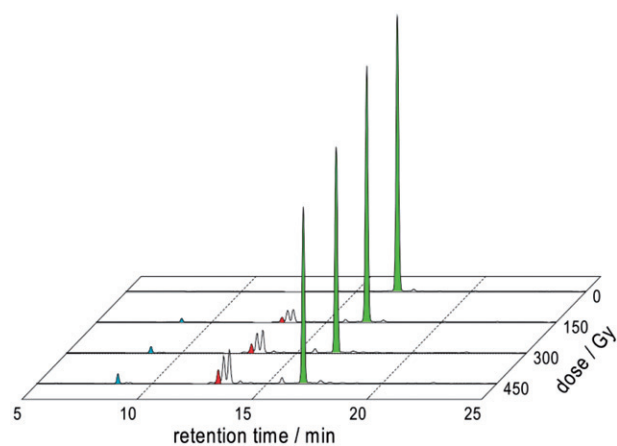


Figure 5. HPLC traces of γ -irradiated of $\text{N}_2\text{O}:\text{O}_2$ (90:10 v/v)-saturated solutions of 1.10 mM Gly-Met-Gly at natural pH (dose rate $\sim 5.5 \text{ Gy min}^{-1}$) after OPA derivatization.

Table 3. G -values calculated from the HPLC analyses of γ -irradiated $\text{N}_2\text{O}:\text{O}_2$ (90:10 v/v)-saturated solutions (oxygenated) or N_2O -saturated solutions (deaerated) of 1.10 mM Gly-Met-Gly at natural pH (dose rate $\sim 5.5 \text{ Gy min}^{-1}$) after OPA derivatization.

Compound or retention time (R_t)	Oxygenated solutions ^a $G, \mu\text{mol J}^{-1}$	Deaerated solutions ^b $G, \mu\text{mol J}^{-1}$
Gly-Met-Gly	-0.640	-0.460
$R_t = 8.7 \text{ min}$	0.042	^c
Gly-Met(O)-Gly	0.053	0.003
$R_t = 13.2 \text{ min}$	0.242	0.024
$R_t = 13.4 \text{ min}$	0.249	0.032
$R_t = 14.5 \text{ min}$	^c	0.020
$R_t = 15.7 \text{ min}$	0.015	0.007

^a $\text{N}_2\text{O}:\text{O}_2$ (90:10 v/v)-saturated solutions.

^b N_2O -saturated solutions.

^cNo detected.

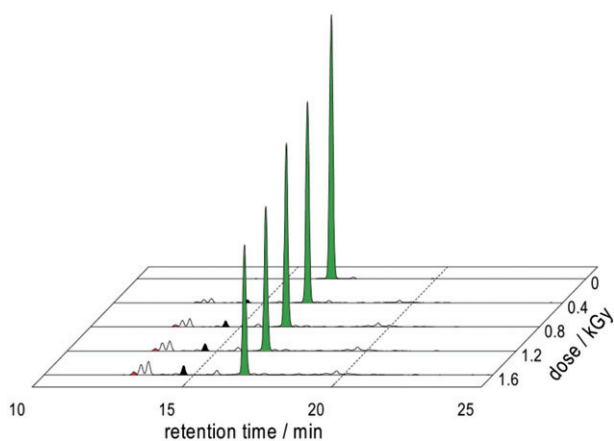


Figure 6. HPLC traces of γ -irradiation of N_2O -saturated solutions of 1.10 mM Gly-Met-Gly at natural pH (dose rate $\sim 5.5 \text{ Gy min}^{-1}$) after OPA derivatization.

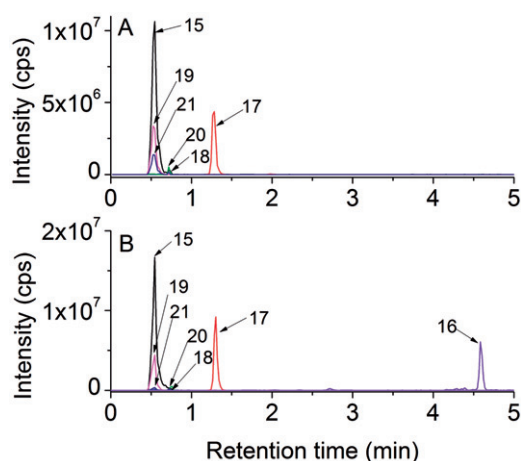


Figure 7. LC-MS analyses of γ -irradiated solutions of 1.10 mM Gly-Met-Gly at natural pH: (A) $N_2O:O_2$ (90:10 v/v)-saturated at a dose of 450 Gy; (B) N_2O -saturated at a dose of 1600 Gy.

$G(\text{HO}^\bullet) = 0.55 \mu\text{mol J}^{-1}$; that is, HO^\bullet radicals and H^\bullet atoms account for 90 and 10% of the reactive species [47,48]. N_2O -saturated solutions containing Gly-Met-Gly (1.10 mM) at natural pH were irradiated under stationary state conditions with a dose rate of ca. 5.5 Gy min^{-1} followed by OPA derivatization of amino compounds and HPLC analysis [9]. The consumption of Gly-Met-Gly (green peaks, Figure 6) led to the formation of five new products, three major and two minor ones. The product that eluted first from the column ($R_t = 12.9 \text{ min}$, red peaks) was identified as Gly-Met(O)-Gly by comparison with the corresponding OPA derivatives obtained from Gly-Met-Gly oxidation by H_2O_2 . It is worth underline that the reaction in the absence of oxygen leads to the formation of three products with retention times 13.2 min, 13.4 min, and 15.7 min which are also present when the reaction is carried out in the presence of oxygen (cf. Figures 5 and 6). The HPLC analysis evidenced

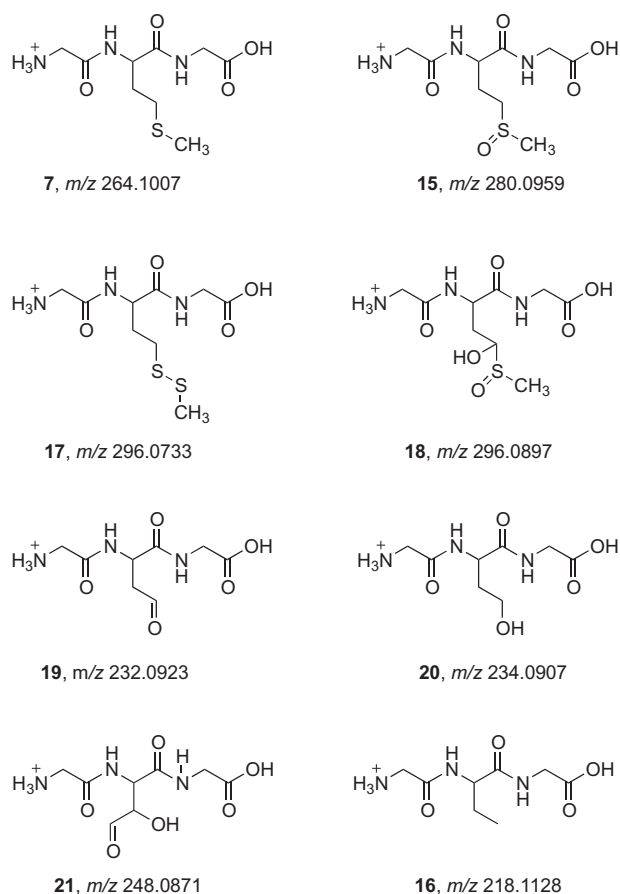


Figure 8. Structures of identified compounds based on high-resolution MS/MS spectra.

the formation of another product with $R_t = 14.5 \text{ min}$, noting that this product is not observed in the reaction in the presence of oxygen. On the other hand, the reaction in the presence of oxygen yielded a product with $R_t = 8.7 \text{ min}$ which is not present in the absence of oxygen.

Based on our previous proteomic studies [23,31], the formation of the product exclusively seen under deoxygenated conditions ($R_t = 14.5 \text{ min}$, Figure 6, black peaks) is expected to be the corresponding tripeptide containing α -aminobutyric acid (compound 16). Therefore, we proceeded analyzing the reaction of H^\bullet with Gly-Met-Gly. For doing so, we studied the γ -irradiation of N_2O -saturated solutions of 1.10 mM Gly-Met-Gly at natural pH (dose rate $\sim 5.5 \text{ Gy min}^{-1}$) containing 0.2 M of *tert*-butanol. In this reaction HO^\bullet radicals are efficiently trapped by *tert*-butanol ($k = 6.0 \times 10^8 \text{ M}^{-1} \text{ s}^{-1}$). Samples were withdrawn at a dose of 1.6 kGy followed by OPA derivatization and HPLC analysis. Under these reaction conditions the formation of a product with $R_t = 14.5 \text{ min}$ as well as of Gly-Met(O)-Gly was observed. The irradiated samples were also analyzed by ESI-MS (positive mode), verifying the presence of three

compounds in the reaction mixture identified by their masses, i.e. m/z 264.1 corresponding to **7** + 1, m/z 280.1 corresponding to **15** + 1 and m/z 218.1 corresponding to **16** + 1.

Analysis of the data from the experiment reported in Figure 6 in terms of chemical radiation yields afforded a G value for the production of **16** of $0.02 \mu\text{mol J}^{-1}$ which is one third of $G(\text{H}^\bullet) = 0.06 \mu\text{mol J}^{-1}$. The G values for the consumption of Gly-Met-Gly and formation of the products bearing the primary amine functionality detectable by OPA – HPLC technique are shown in Table 3. The G for the consumption of Gly-Met-Gly is -0.460 and the sum of the G -values of all the products detected is 0.086 . Comparison of these values suggests formation of the products that lose the amine functionality. It is worth underlining that in the presence of oxygen the radiation chemical yields (G -values) are quite different (see Table 3).

LC-MS and high-resolution MS/MS

The HPLC analyses of the samples irradiated in the absence or presence of oxygen are shown in Figure 7. In agreement with the OPA derivatization, it is clear that, including the starting material, six compounds are present in the two experiments whereas an extra peak is observed in the absence of oxygen. All peaks were identified and assigned to the structures in Figure 8 by their high resolution mass data together with their characteristic fragmentation patterns as shown in Figures 9 and 10.

The high resolution MS/MS spectrum of the starting material **7** (mw 264.1007 Da) and the spectra of three other products with higher molecular weights are shown in Figure 9. The accurate masses of these products, m/z 280.0959, 296.0897, 296.0733, correspond to a molecular weight increase equivalent to atomic masses of one oxygen atom, two oxygen atoms and one sulfur atom, respectively, as compared to the starting material. By an independent synthesis using hydrogen peroxide oxidation, the sulfoxide and sulfone of the tripeptide were obtained, confirming the assignment of compound **15** as the sulfoxide. The location of the two oxygen atoms of the m/z 296.0897 product (compound **18**) could not be derived from the MS/MS spectrum. However, the retention time of the authentic sulfone was 0.7 min while that of compound **18** was 1.3 min so this product cannot be assigned to the sulfone. The structure of compound **18** will be further discussed in the paper in the mechanistic proposal. The m/z 296.0733 product with the addition of a sulfur atom was assigned to compound **17** by the characteristic fragmentation of an asymmetrical disulfide. It is worth

underlining that this is the major product of the tripeptide transformation.

The high resolution MS/MS spectra of the products with lower molecular weight compared to the starting material are shown in Figure 10. These products are assigned to compounds where the Met residue has lost the CH_3S moiety. The compound with mass m/z 218.1128 was assigned to the conversion of Met residue into α -aminobutyric acid (compound **16**) that is formed only in the absence of oxygen (cf. Figure 7). The other three compounds were identified by their high-resolution MS/MS fragment ions as compounds **19**, **20**, and **21**, for which the mechanistic steps of their formation will be further discussed.

Electrochemical oxidation of Gly-Met-Gly

Electrochemical oxidation of peptides readily occurs at tyrosine (Tyr), tryptophan (Trp), and Met [49], while hydroxyl-radical-mediated oxidations occur at phenylalanine (Phe) [42], which has been used in protein and peptide chemistry [50–52]. We have recently reported that both direct oxidation and hydroxyl radical-mediated oxidation of peptides can be achieved in thin-layer (amperometric) flow cells with boron doped diamond (BDD) electrodes [42]. The specific property of BDD to generate HO^\bullet by oxidation of water (when used as a working electrode at high potential) is favorable for studying the oxidation of Gly-Met-Gly peptide and mimicking its radiolytically induced oxidation.

In this work, electrochemical direct oxidation and HO^\bullet -induced oxidation of Gly-Met-Gly were studied by using a linear potential sweep in an on-line EC-MS experiment. The measured mass-voltammograms allowed monitoring of specific oxidation and corresponding products at different potentials. A decrease of the Gly-Met-Gly signal (Figure 11) indicated the onset of electrochemical oxidation at ~ 800 mV. Oxidation efficiency increased further with increasing working electrode potential, reaching an oxidation yield of $>75\%$ at potentials higher than 1200 mV, which was determined from a decrease in Gly-Met-Gly signal intensity. Signal intensity for the oxidation product (Gly-Met(O)-Gly) reached a maximum at 1200 mV, followed by a decrease at higher potentials (Figure 11(B)) likely due to the formation of Gly-Met(O_2)-Gly. It is clearly shown that formation of Gly-Met(O_2)-Gly started from ~ 1200 mV and increased until 2500 mV, after which the signal intensity slightly decreased to a stable range of the voltammogram from 2500 to 3000 mV (Figure 11(C)). We have shown that generation of OH-radicals occurs at potentials higher than 2000 mV on BDD electrode in this cell, using LFL oxidation as the readout [35]. The formation

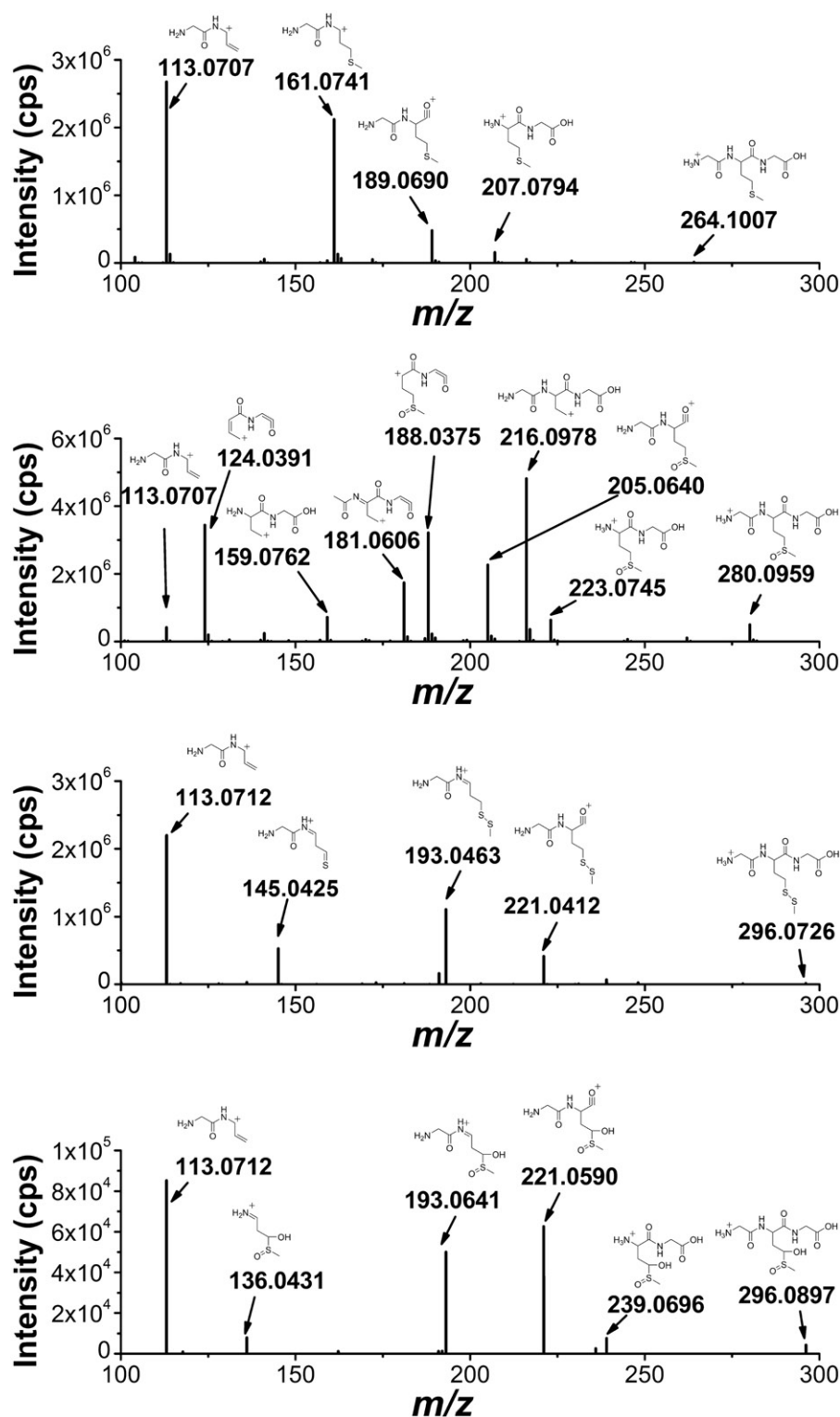


Figure 9. High-resolution MS/MS spectra of starting material 7 (m/z 264.1007) and of the products with higher molecular weight 15 (m/z 280.0959), 17 (m/z 296.0733), and 18 (m/z 296.0897) with proposed structures of the fragment ions.

of Gly-Met(O₂)-Gly occurred based on further oxidation of Gly-Met(O)-Gly, indicated by the consuming of Gly-Met(O)-Gly from 1200 mV to 2500 mV. Since the potential of 1200 mV is much lower than the hydroxyl radical

generating potential and since more than 75% of substrate has been converted at a potential of 1200 mV, the conversion of Gly-Met-Gly to Gly-Met(O)-Gly can be attributed to H₂O₂ generation at the BDD electrode.

γ -irradiation of Gly-Met-Gly in deoxygenated POPC vesicles: the role of thiyl radicals

The biomimetic model of a cell membrane consisted of 1 mM suspensions of 1-palmitoyl-2-oleoylphosphatidylcholine (POPC) liposomes in the form of large unilamellar vesicles (LUVET) containing the *cis* monounsaturated fatty acid residues, to which solutions of Gly-Met-Gly at

natural pH were added to reach a final concentration of 100 μ M. A set of four vials was prepared and the mixtures were saturated with N_2O prior to γ -irradiation for 25, 50, 100, and 150 Gy, respectively. Each vial was irradiated at the specified dose followed by lipid isolation and derivatization to the corresponding fatty acid methyl esters, and the *cis/trans* lipid isomer

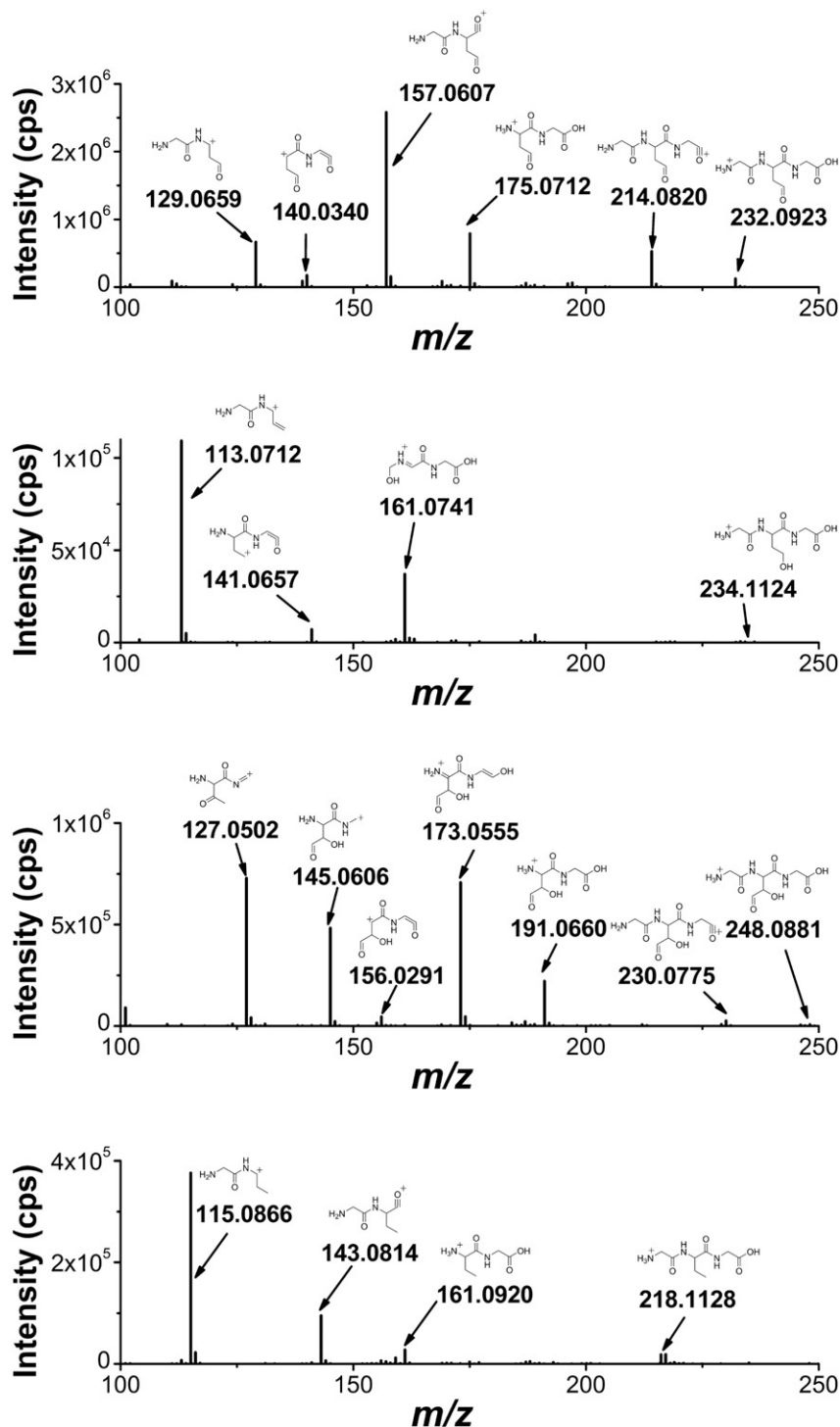


Figure 10. High-resolution MS/MS spectra of the products with lower molecular weight than the starting tripeptide: 19 (m/z 232.0923), 20 (m/z 234.0907), 21 (m/z 248.0871), and 16 (m/z 218.1128) with proposed structures of the fragment ions.

ratio was determined by GC analyses. Control experiments in the absence of Gly-Met-Gly showed no detectable amounts of elaidate after exposure to 250 Gy. In all experiments, the geometrical isomer-

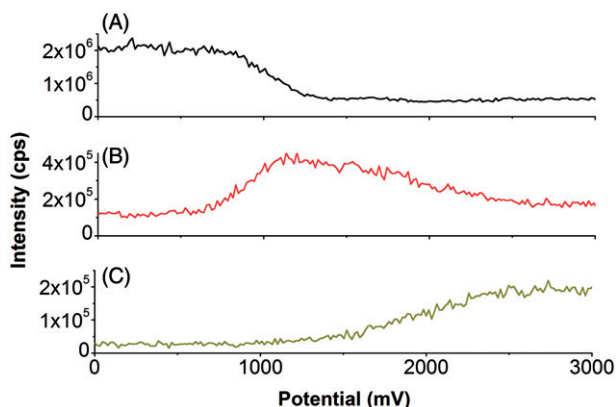
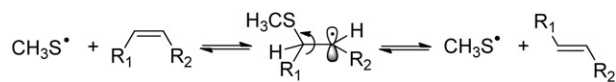


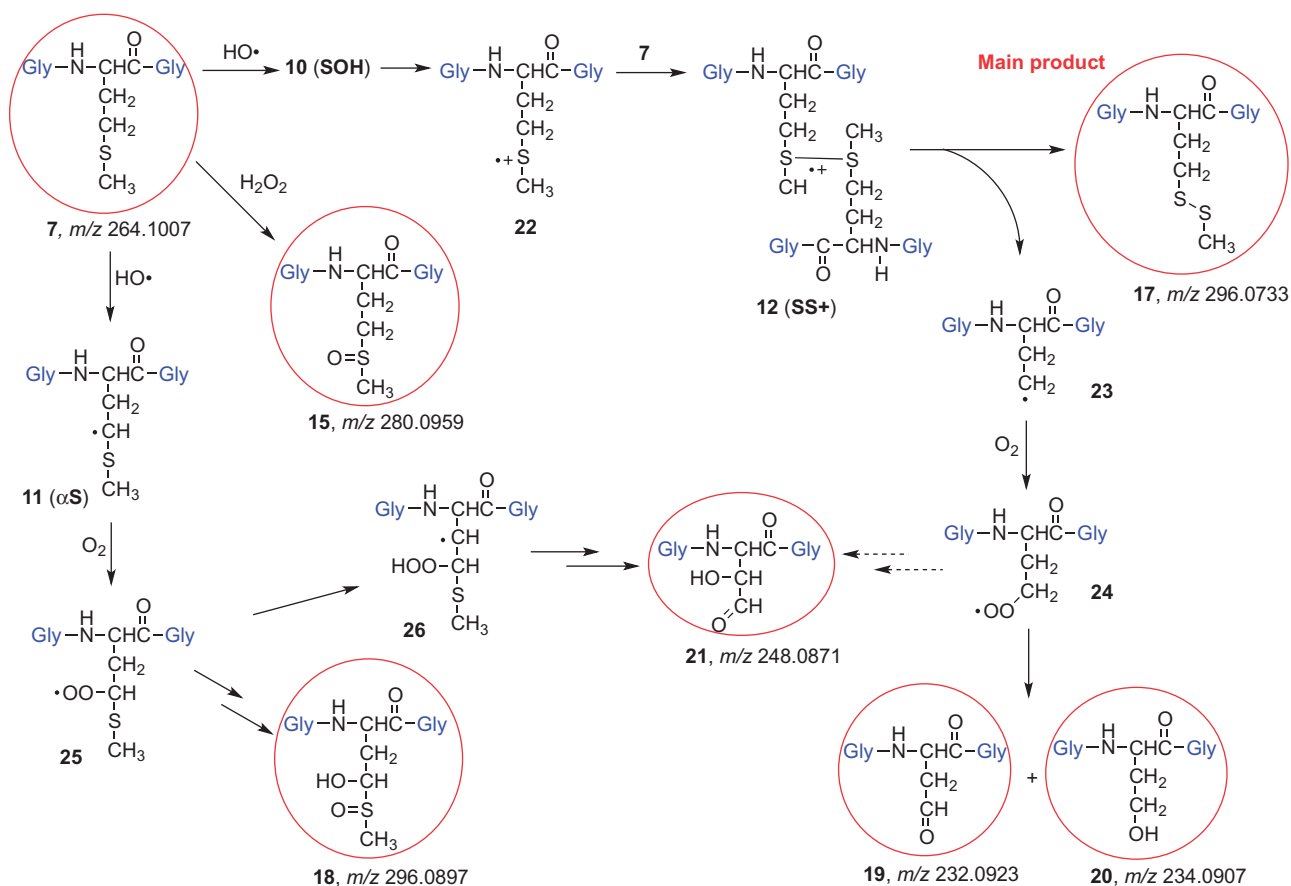
Figure 11. On-line mass-voltammograms of Gly-Met-Gly electrochemical oxidation. On-line mass-voltammograms of Gly-Met-Gly (20 μ M in 89/10/1 (v/v/v) water/acetonitrile/formic acid) were recorded by ramping the potential from 0 to 4000 mV with a scan rate of 20 mV/s. Traces were extracted and plotted versus cell potential for A: Gly-Met-Gly, B: Gly-Met(O)-Gly and C: Gly-Met(O₂)-Gly.

ization of the unsaturated lipid chain of the POPC vesicle occurred and the formation of elaidate (*trans* isomer) increased as the dose increases (see Table S10 in Supporting Information). Similar experiment by adding 0.2 M *tert*-butanol in order to trap HO[•] radicals showed very similar results.

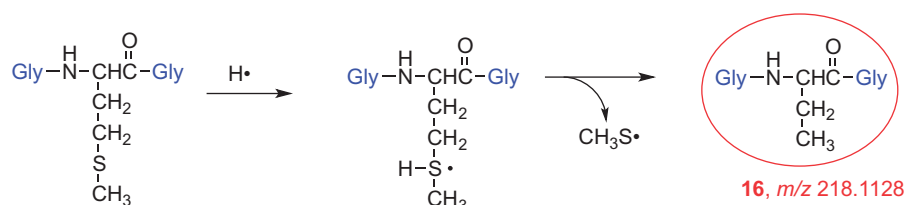
After 25 Gy a 31.5% of elaidate was formed, reaching 82.4% after 150 Gy, which is close to the *trans/cis* ratio at thermodynamic equilibrium. Based on previous investigations [23,31], these findings can be explained by the occurrence of peptide desulfurization processes, generating diffusible CH₃S[•] radicals from Gly-Met-Gly, which are able to migrate from the aqueous phase to the membrane bilayer, and transform the double bond of the oleate moiety by the catalytic addition-elimination mechanism shown in Scheme 5.



Scheme 5. Reaction mechanism for the *cis-trans* isomerization catalyzed by CH₃S[•] radicals.



Scheme 6. Proposed mechanism for the reaction of HO[•] radicals with Gly-Met-Gly (7).



Scheme 7. Proposed mechanism for the formation of α -aminobutyric moiety (**16**).

Overall mechanism proposal

Our analytical approach allowed us proposing the mechanism of Gly-Met-Gly (**7**) transformation by radiolysis based on product identification. First, using the parallel radiolytical and electrochemical oxidation protocols we could unequivocally demonstrate that the formation of the sulfoxide **15** is not due to direct hydroxyl radical reactivity, but to the *in situ* generation of hydrogen peroxide (Scheme 6). In fact, we recall that **15** was found also when the DBB potential was around 1200 mV, that is lower than the HO \cdot radical generating potential.

From pulse radiolysis the most important reaction of HO \cdot radicals with **7** is the formation of adduct radical **10** (SOH), which undergoes a variety of transformation (cf. Scheme S1). As far as the product identification from the Met moiety is concerned, the most relevant reactivities are: (i) the H-abstraction of the CH₂-S moiety to give the intermediate **11** (α S), (ii) the HO \cdot radical addition to give **10** (SOH) followed by HO $^-$ elimination to give the sulfide radical cation **22** (Scheme 6). This latter intermediate can react with another molecule of tripeptide **7**, to give the disulfide radical cation **12** (SS $^+$). We suggest that **12** fragments and affords the observed disulfide **17**, which is the main product, and the alkyl radical **23**. The primary alkyl radical **23** can react with molecular oxygen giving the peroxy radical **24** that decay via the recombination process. The resulting tetroxide intermediate decay into products **19** and **20** (Scheme 6) [53].

The intermediate **11** can react with oxygen to give the peroxy radical **25**. We suggest that it can be reduced to peroxide (e.g. by the radical **8** which is a good electron donor) and internally give sulfide oxidation, then reducing it to alcohol **18**. The product **21** can derive from the peroxy radical **25** and/or **24**, e.g. through an intramolecular H-transfer with a five-membered transition state, giving the alkyl radical **26**, then via internal homolytic substitution affording an alkoxy radical that further eliminate MeS \cdot and the aldehyde **21**.

Finally, only in the absence of oxygen, the H \cdot atom addition to the Met moiety and formation of a

sulfuranyl radical intermediate occurs also in this tripeptide substrate, as known already for the amino acid Met, thus bringing to α -aminobutyric moiety **16** (Scheme 7) [23,31]. Furthermore, the sulfuranyl radical can produce a diffusible MeS \cdot radical that is known to give other reactions, such as to migrate to the membrane phospholipid bilayer and catalyze the *cis* to *trans* double bond isomerization (see Scheme 5).

Conclusions

The present study offers a multi-methodological approach to contribute to solve the most intriguing free radical-based mechanisms involving Met. Generation of radical species through parallel methodologies, such as radiolysis and electrochemistry, provided strong evidence that Met oxidation in the tripeptide derives from the *in situ* formed hydrogen peroxide. It is relevant that the main product of the tripeptide is an unsymmetrical disulfide obtained by the dimerization of an intermediate sulfur radical cation. The use of aerobic conditions highlighted the formation of other products derived from peroxy radicals of the tripeptide, as well as the desulfurization with formation of diffusible thiyl radicals.

This model study provides new hints in free radical research applied to biomolecules and is expected to inspire proteomic studies of oxidative protein damage.

Acknowledgements

All authors gratefully acknowledge the support and networking opportunities they received from COST Action CM1201 on "Biomimetic Radical Chemistry". One of us (KB) would like to thank Professor Ian Carmichael for his hospitality during the stay. This is document number NDRL-5130 from the Notre Dame Radiation Laboratory.

Disclosure statement

The authors report no conflicts of interest. The authors alone are responsible for the content and writing of this article.

Funding

This publication is based on the work of COST Action CM1201, supported by COST (European Cooperation in Science and Technology) U.S. Department of Energy Office of Science [DE-FC02-04ER15533].

References

- Poole LB, Karplus PA, Claiborne A. Protein sulfenic acids in redox signaling. *Annu Rev Pharmacol Toxicol* 2004;44:325–347.
- Weissbach H, Resnick L, Brot N. Methionine sulfoxide reductases: history and cellular role in protecting against oxidative damage. *Biochim Biophys Acta* 2005;1703:203–212.
- Lu S, Levine RL. Methionine in proteins defends against oxidative stress. *FASEB J* 2009;23:464–472.
- Stadtman ER, Van Remmen H, Richardson A, Wehr NB, Levine RL. Methionine oxidation and aging. *Biochim Biophys Acta* 2005;1703:135–140.
- Davies MJ. The oxidative environment and protein damage. *Biochim Biophys Acta* 2005;1703:93–109.
- Davies MJ, Fu S, Wang H, Dean RT. Stable markers of oxidant damage to proteins and their application in the study of human disease. *Free Radic Biol Med* 1999;27:1151–1163.
- Jensen JL, Miller BL, Zhang X, Hug GL, Schoneich C. Oxidation of threonylmethionine by peroxyxynitrite. Quantification of the one-electron transfer pathway by comparison to one-electron photooxidation. *J Am Chem Soc* 1997;119:4749–4757.
- Schoneich C. Methionine oxidation by reactive oxygen species: reaction mechanisms and relevance to Alzheimer's disease. *Biochim Biophys Acta* 2005;1703:111–119.
- Barata-Vallejo S, Ferreri C, Postigo A, Chatgililoglu C. Radiation chemical studies of methionine in aqueous solution: understanding the role of molecular oxygen. *Chem Res Toxicol* 2010;23:258–263.
- Hiller K-O, Masloch B, Göbl M, Asmus K-D. Mechanism of the OH[•] radical induced oxidation of methionine in aqueous solution. *J Am Chem Soc* 1981;103:2734–2743.
- Hiller K-O, Asmus K-D. Formation and reduction reactions of α -amino radicals derived from methionine and its derivatives in aqueous solutions. *J Phys Chem* 1983;87:3682–3688.
- Glass RS, Hug GL, Schoneich C, Wilson GS, Kuznetsova L, Lee T, et al. Neighboring amide participation in thioether oxidation: relevance to biological oxidation. *J Am Chem Soc* 2009;131:13791–13805.
- Bobrowski K, Holcman J. Formation and stability of intramolecular three-electron S \cdot :N, S \cdot :S and S \cdot :O bonds in one-electron-oxidized simple methionine peptides. Pulse radiolysis study. *J Phys Chem* 1989;93:6381–6387.
- Schoneich C, Pogocki D, Wisniowski P, Hug GL, Bobrowski K. Intramolecular sulfur-oxygen bond formation in radical cations of N-acetylmethionine amide. *J Am Chem Soc* 2000;122:10224–10225.
- Schoneich C, Pogocki D, Hug GL, Bobrowski K. Free radical reactions of methionine in peptides: mechanisms relevant to beta-amyloid oxidation and Alzheimer's disease. *J Am Chem Soc* 2003;125:13700–13713.
- Bobrowski K, Hug GL, Pogocki D, Marciniak B, Schoneich C. Stabilization of sulfide radical cations through complexation with the peptide bond: mechanisms relevant to oxidation of proteins containing multiple methionine residues. *J Phys Chem B* 2007;111:9608–9620.
- Ohara A. On the radiolysis of methionine in aqueous solution by gamma irradiation. *J Radiat Res* 1966;7:18–27.
- Xu G, Chance MR. Radiolytic modification of sulfur containing amino acid residues in model peptides: fundamental studies for protein footprinting. *Anal Chem* 2005;77:2437–2449.
- Ignasiak M, Scuderi D, de Oliveira P, Pedzinski T, Rayah Y, Houée Levin C. Characterization by mass spectrometry and IRMPD spectroscopy of the sulfoxide group in oxidized methionine and related compounds. *Chem Phys Lett* 2011;502:29–36.
- Ignasiak M, de Oliveira P, Houée Levin C, Scuderi D. Oxidation of methionine-containing peptides by OH radicals: is sulfoxide the only product? Study by mass spectrometry and IRMPD spectroscopy. *Chem Phys Lett* 2013;590:35–40.
- Miller BL, Kuczera K, Schoneich C. One-electron photo-oxidation of N-methionyl peptides. Mechanism of sulfoxide and azasulfonium diastereomer formation through reaction of sulfide radical cation complexes with oxygen or superoxide. *J Am Chem Soc* 1998;120:3345–3356.
- Bonifacic M, Hug GL, Schoneich C. Kinetic of the reactions between sulfide radical cation complexes [S \cdot :S]⁺ and [S \cdot :N]⁺, and superoxide or carbon dioxide radical anions. *J Phys Chem A* 2000;104:1240–1245.
- Chatgililoglu C, Ferreri C, Torreggiani A, Renzone G, Salzano AM, Scaloni A. Radiation-induced reductive modifications of sulfur-containing amino acids within peptides and proteins. *J Proteomics* 2011;74:2263–2273.
- Chatgililoglu C, Ferreri C, Masi A, Melchiorre M, Sansone A, Terzidis MA, Torreggiani A. Biomimetic models of radical stress and related biomarkers. *Chimia* 2012;66:368–371.
- Mozziconacci O, Bobrowski K, Ferreri C, Chatgililoglu C. Reactions of hydrogen atoms with met-enkephalin and related peptides. *Chemistry* 2007;13:2029–2033.
- Kadlcik V, Sicard-Roselli C, Houée-Levin C, Kodicek M, Ferreri C, Chatgililoglu C. Reductive modification of a methionine residue in the amyloid-beta peptide. *Angew Chem Int Ed Engl* 2006;45:2595–2598.
- Ferreri C, Manco I, Faraone-Mennella MR, Torreggiani A, Tamba M, Manara S, Chatgililoglu C. The reaction of hydrogen atoms with methionine residues: a model of reductive radical stress causing tandem protein-lipid damage. *ChemBioChem* 2006;7:1738–1744.
- Ferreri C, Chatgililoglu C, Torreggiani A, Salzano AM, Renzone G, Scaloni A. The reductive desulfurization of Met and Cys residues in bovine RNase A associated with the trans lipid formation in a mimetic model of

- biological membranes. *J Proteome Res* 2008;7:2007–2015.
29. Salzano AM, Renzone G, Scaloni A, Torreggiani A, Ferreri C, Chatgililoglu C. Human serum albumin modifications associated with reductive radical stress. *Mol BioSyst* 2011;7:889–898.
 30. Torreggiani A, Domènech J, Ferreri C, Orihuela R, Atrian S, Capdevila M, Chatgililoglu C. Zinc and cadmium complexes of a plant metallothionein under radical stress: desulfurisation reactions associated with the formation of trans lipids in model membranes *Chem Eur J* 2009;15:6015–6024.
 31. Chatgililoglu C, Ferreri C, Melchiorre M, Sansone A, Torreggiani A. Lipid geometrical isomerism: from chemistry to biology and diagnostics. *Chem Rev* 2014;114:255–284.
 32. Hug GL, Wang Y, Schöneich C, Jiang P-Y, Fessenden RW. Multiple time scale in pulse radiolysis. Application to bromide solutions and dipeptides. *Radiat Phys Chem* 1999;54:559–566.
 33. Janata E, Schuler RH. Rate constant for scavenging e_{aq}^- in N_2O -saturated solutions. *J Phys Chem* 1982;86:2078–2084.
 34. Bevington PR. Data reduction and error analysis for the physical sciences. New York: McGraw-Hill; 1969.
 35. Marciniak B, Bobrowski K, Hug GL. Quenching of triplet states of aromatic ketones by sulfur-containing amino acids in solution. Evidence for electron transfer. *J Phys Chem* 1993;97:11937–11943.
 36. Schöneich C, Bobrowski K. Intramolecular hydrogen transfer as the key step in the dissociation of hydroxyl radical adducts of (alkylthio)ethanol derivatives. *J Am Chem Soc* 1993;115:6538–6547.
 37. Pogocki DM. Investigation of radical processes induced by hydroxyl radical in amino acids and peptides containing thioether group. In: Department of Radiation Chemistry and Technology. Warsaw, Poland: Institute of Nuclear Chemistry and Technology; 1996.
 38. Asmus K-D, Göbl M, Hiller K-O, Mahling S, Mönig J. S.:N and S.:O three-electron-bonded radicals and radical cations in aqueous solutions. *J Chem Soc Perkin Trans* 1985;2:641–646.
 39. Hiller K-O, Asmus K-D. Tl^{2+} and Ag^{2+} metal-ion-induced oxidation of methionine in aqueous solution. A pulse radiolysis study. *Int J Radiat Biol Relat Stud Phys Chem Med* 1981;40:597–604.
 40. Mieden OJ, von Sonntag, C. Peptide free-radicals: the reactions of OH radicals with glycine anhydride and its methyl derivatives sarcosine and alanine anhydride. A pulse radiolysis and product study. *Z Naturforsch* 1989;44b:959–974.
 41. Spinks JWT, Woods RJ. An introduction to radiation chemistry. 3rd ed. New York: Wiley; 1990:100.
 42. Roeser J, Alting NFA, Permentier HP, Bruins AP, Bischoff R. Boron-doped diamond electrodes for the electrochemical oxidation and cleavage of peptides. *Anal Chem* 2013;85:6626–6632.
 43. Bobrowski K, Hug GL, Pogocki D, Marciniak B, Schöneich C. Sulfur radical cation-peptide bond complex in the one-electron oxidation of S-methylglutathione. *J Am Chem Soc* 2007;129:9236–9245.
 44. Greene J, Henderson JW Jr, Wikswow JP. Rapid and precise determination of cellular amino acid flux rates using HPLC with automated derivatization with absorbance detection. Agilent Technologies; 2009. <https://www.chem.agilent.com/Library/applications/5990-3283EN.pdf>.
 45. Bartolomeo M P, Maisano F. Validation of a reversed phase HPLC method for quantitative amino acid analysis. *J Biomol Tech* 2006;17:131–137.
 46. Bielski BH, Cabelli DE, Arudi RL, Ross AB. Reactivity of HO_2/O_2^- radicals in aqueous solution. *J Phys Chem Ref Data* 1985;14:1041–1051.
 47. Buxton GV, Greenstock CL, Helman WP, Ross AB. Critical review of rate constants for reactions of hydrated electron, hydrogen atoms and hydroxyl radicals ($(^{\bullet}OH)/^{\bullet}O^-$) in aqueous solution. *J Phys Chem Ref Data* 1988;17:513–886.
 48. Ross AB, Mallard WG, Helman WP, Buxton GV, Huie RE, Neta P. NDRLNIST Solution Kinetic Database Ver. 3, Notre Dame Radiation Laboratory and NIST Standard Reference Data, Notre Dame, IN, and Gaithersburg, MD; 1998.
 49. Roeser J, Permentier HP, Bruins AP, Bischoff R. Electrochemical oxidation and cleavage of tyrosine- and tryptophan-containing tripeptides. *Anal Chem* 2010;82:7556–7565.
 50. Permentier HP, Jurva U, Barroso B, Bruins AP. Electrochemical oxidation and cleavage of peptides analyzed with on-line mass spectrometric detection. *Rapid Commun Mass Spectrom* 2003;17:1585–1592.
 51. Permentier HP, Bruins AP. Electrochemical oxidation and cleavage of proteins with on-line mass spectrometric detection: development of an instrumental alternative to enzymatic protein digestion. *J Am Soc Mass Spectrom* 2004;15:1707–1716.
 52. Herzog G, Arrigan DWM. Electrochemical strategies for the label-free detection of amino acids, peptides and proteins. *Analyst* 2007;132:615–632.
 53. von Sonntag C. Free-radical-induced DNA damage and its repair: a chemical perspective. Berlin: Springer-Verlag; 2006:160–194, Chapter 8.